

Interactions of the doubly charmed state T_{cc}^+ with a hadronic medium

L. M. Abreu* and H. P. L. Vieira†
Instituto de Física, Universidade Federal da Bahia,
Campus Universitário de Ondina, 40170-115, Bahia, Brazil

F. S. Navarra‡
Instituto de Física, Universidade de São Paulo, Rua do Matão, 1371, CEP 05508-090, São Paulo, SP, Brazil

The recently observed doubly charmed state T_{cc}^+ belongs to the family of the multiquark states called exotic hadrons. One of main goals of modern hadron physics is to determine the structure of these exotic hadrons. Nucleus-nucleus collisions at the LHC offer a possibility to achieve this goal. The yield of T_{cc}^+ 's produced at the end of the quark-gluon plasma phase of nuclear collisions is related to the internal structure of the state. However this yield may be affected by the interactions in the hadron gas phase. We investigate the absorption and production processes of this new state in a hadronic medium, considering the reactions $T_{cc}^+\pi, T_{cc}^+\rho \rightarrow D^{(*)}D^{(*)}$ and the corresponding inverse reactions. We use effective field Lagrangians to account for the couplings between light and heavy mesons. The absorption cross sections are found to be larger than the production ones. We compare our results with the only existing estimate of these quantities, presented in a work of J. Hong, S. Cho, T. Song and S. H. Lee, in which the authors employed the quasi-free approximation. We find cross sections which are one order of magnitude smaller. The subject deserves further investigation.

I. INTRODUCTION

Very recently the LHCb collaboration has reported the observation of a narrow peak in the $D^0D^0\pi^+$ -mass spectrum in proton-proton (pp) collisions with statistical significance of more than 10σ [1, 2]. By using an amplitude model based on the Breit-Wigner formalism, this peak has been fitted to one resonance with a mass of approximately 3875 MeV and quantum numbers $J^P = 1^+$. Its minimum valence quark content is $cc\bar{u}\bar{d}$, giving it the unequivocal status of the first observed unconventional hadron with two heavy quarks of the same flavor. According to the data, its binding energy with respect to the $D^{*+}D^0$ mass threshold is $273 \pm 61 \pm 5_{-14}^{+11}$ keV and the decay width is $410 \pm 165 \pm 43_{-38}^{+18}$ keV. These values are consistent with the expected properties for a T_{cc}^+ isoscalar tetraquark ground state with $J^P = 1^+$.

Even before the experimental discovery of this doubly charmed tetraquark state, there was a debate concerning its fundamental aspects, such as its decay/formation mechanisms and underlying structure [3–14]. Its discovery obviously stimulated the appearance of more studies employing different theoretical approaches [15–27]. In particular, several works have investigated the implications of the T_{cc}^+ structure (hadron molecule or compact tetraquark) for the observables. However, a compelling understanding of the nature of the T_{cc}^+ is still lacking.

In order to determine the internal structure of the T_{cc}^+ state, more detailed experimental data and theoretical studies are necessary. In this context, heavy-ion collisions appear as a promising environment, where charm

quarks are copiously produced. The search for exotic charm hadrons in heavy-ion collisions has already started and the $X(3872)$ has been observed by the CMS and LHCb collaborations. In these collisions there is a phase transition from nuclear matter to the quark-gluon plasma (QGP), i.e. the locally thermalized state of deconfined quarks and gluons. The QGP expands, cools down and hadronizes, forming a gas of hadrons. When this last transition takes place, heavy quarks coalesce to form multiquark bound states at the end of the QGP phase. Next, the multiquark states interact with other hadrons in the course of the hadronic phase. They can be destroyed in collisions with the comoving light mesons, or produced through the inverse processes [28–36]. The final yields depend on the hadronic interactions which, in turn, depend on the spatial configuration of the multiquark systems. Therefore, the evaluation of the interaction cross sections of the T_{cc} with light mesons is a crucial ingredient for the interpretation of the data. While the hadronic interactions of the $X(3872)$ have been addressed in several papers, there is only one work, [11], where the T_{cc} - light meson cross section was calculated. In Ref. [11] the authors treated the T_{cc} as a loosely bound state of a D and a D^* . In this approach it seems natural to use the quasi-free approximation, in which the charm mesons are taken to be on-shell and their mutual interaction and binding energy are neglected. In the quasi-free approximation the T_{cc} is absorbed when a pion from hadron gas interacts with the D or with the D^* . In each of these interactions the other heavy meson is a spectator. The advantage of this approach is that the only dynamical ingredient is the $D^*D\pi$ Lagrangian, which is well-known. On the other hand, the role of the quantum numbers of the D^*D bound state is neglected. Moreover, some possible final states are not included. Clearly the subject deserves further investigation and this is the main purpose of this work.

* luciano.abreu@ufba.br

† hilde_son@hotmail.com

‡ navarra@if.usp.br

In what follows we will evaluate the hadronic effects on the T_{cc}^+ state. We will make use of Effective Lagrangians to calculate the cross sections of the processes $T_{cc}^+\pi, T_{cc}^+\rho \rightarrow D^{(*)}D^{(*)}$, as well as those of the corresponding inverse processes. These cross sections may be used to estimate how the abundance of this exotic state is changed during the hadron gas phase of heavy ion collisions.

The paper is organized as follows. In Section II we describe the effective formalism and introduce the cross sections of the T_{cc}^+ -absorption and production reactions. In Section III we present and analyze the results obtained. Finally, Section IV is devoted to the summary of the main points and to the concluding remarks.

II. FRAMEWORK

We are interested in the interactions of the T_{cc}^+ state with the surrounding hadronic medium composed of the lightest pseudoscalar and vector mesons, i.e. π and ρ mesons, respectively. Because of their large multiplicity (mainly the pions) with respect to other light hadrons, the reactions involving them are expected to provide the main contributions. In particular, we focus on the reactions $T_{cc}^+\pi \rightarrow D^{(*)}D^{(*)}$ and $T_{cc}^+\rho \rightarrow D^{(*)}D^{(*)}$, as well as the inverse processes. In Fig. 1 we show the lowest-order Born diagrams contributing to each process, without the specification of the particle charges.

To calculate the respective cross sections related to the reactions in Fig. 1, we make use of the effective hadron Lagrangian approach. Accordingly, for the diagrams (a) – (f) we employ the effective Lagrangians involving π , ρ , D and D^* mesons given by [28–32],

$$\begin{aligned} \mathcal{L}_{\pi DD^*} &= ig_{\pi DD^*} D_\mu^* \vec{\tau} \cdot (\bar{D} \partial^\mu \vec{\pi} - \partial^\mu \bar{D} \vec{\pi}) + h.c., \\ \mathcal{L}_{\rho DD} &= ig_{\rho DD} (D \vec{\tau} \partial_\mu \bar{D} - \partial_\mu D \vec{\tau} \bar{D}) \cdot \vec{\rho}^\mu, \\ \mathcal{L}_{\rho D^* D^*} &= ig_{\rho D^* D^*} [(\partial_\mu D^{*\nu} \vec{\tau} \bar{D}_\nu^* - D^{*\nu} \vec{\tau} \partial_\mu \bar{D}_\nu^*) \cdot \vec{\rho}^\mu \\ &\quad + (D^{*\nu} \vec{\tau} \cdot \partial_\mu \vec{\rho}_\nu - \partial_\mu D^{*\nu} \vec{\tau} \cdot \vec{\rho}_\nu) \bar{D}^{*\mu} \\ &\quad + D^{*\mu} (\vec{\tau} \cdot \vec{\rho}^\nu \partial_\mu \bar{D}_\nu^* - \vec{\tau} \cdot \partial_\mu \vec{\rho}^\nu \bar{D}_\nu^*)], \end{aligned} \quad (1)$$

where $\vec{\tau}$ are the Pauli matrices in the isospin space; $\vec{\pi}$ and $\vec{\rho}$ denote the pion and ρ -meson isospin triplets; and $D^{(*)} = (D^{(*)0}, D^{(*)+})$ represents the isospin doublet for the pseudoscalar (vector) $D^{(*)}$ meson. The coupling constants $g_{\pi DD^*}$, $g_{\rho DD}$ and $g_{\rho D^* D^*}$ are determined from the decay width of D^* and from the relevant symmetries, having the following values [28, 29]: $g_{\pi DD^*} = 6.3$ and $g_{\rho DD} = g_{\rho D^* D^*} = 2.52$.

In the case of the diagrams (g) – (k) in Fig. 1, the vertices involving light and heavy-light mesons are anomalous, and can be described in terms of a gauged Wess-Zumino action [37]. Explicitly, they are

$$\begin{aligned} \mathcal{L}_{\pi D^* D^*} &= -g_{\pi D^* D^*} \varepsilon^{\mu\nu\alpha\beta} \partial_\mu D_\nu^* \pi \partial_\alpha \bar{D}_\beta^*, \\ \mathcal{L}_{\rho DD^*} &= -g_{\rho DD^*} \varepsilon^{\mu\nu\alpha\beta} (D \partial_\mu \rho_\nu \partial_\alpha \bar{D}_\beta^* + \partial_\mu D_\nu^* \partial_\alpha \rho_\beta \bar{D}), \end{aligned} \quad (2)$$

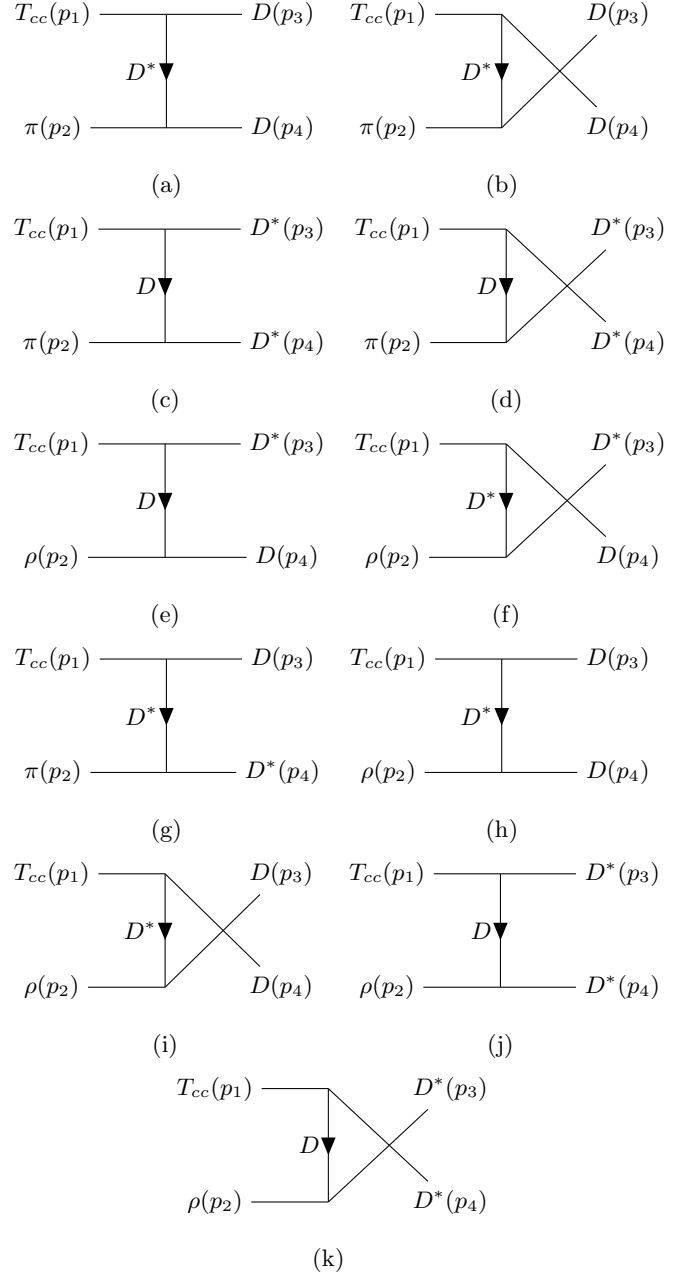


FIG. 1. Diagrams contributing to the following process (without specification of the charges of the particles): $T_{cc}\pi \rightarrow DD$ [(a) and (b)], $T_{cc}\pi \rightarrow D^*D^*$ [(c) and (d)], $T_{cc}\rho \rightarrow D^*D$ [(e) and (f)], $T_{cc}\pi \rightarrow DD^*$ [(g)], $T_{cc}\rho \rightarrow DD$ [(h) and (i)] and $T_{cc}\rho \rightarrow D^*D^*$ [(j) and (k)]. The particle charges are not specified.

with $\epsilon_{0123} = +1$. The coupling constants $g_{\pi D^* D^*}$ and $g_{\rho DD^*}$ have the following values [37]: $g_{\pi D^* D^*} = 9.08 \text{ GeV}^{-1}$ and $g_{\rho DD^*} = 2.82 \text{ GeV}^{-1}$.

In this study, we assume that the T_{cc}^+ is a bound state of D^*D , with quantum numbers $I(J^P) = 0(1^+)$. Therefore, the effective Lagrangian describing the interaction

between the T_{cc} and the DD^* pair is given by [23],

$$\mathcal{L}_{T_{cc}} = ig_{T_{cc}DD^*} T_{cc}^\mu D_\mu^* D. \quad (3)$$

In the expression above, T_{cc} denotes the field associated to T_{cc}^+ state; this notation will be used henceforth. Also, the $D_\mu^* D$ means the $D_\mu^{*+} D^0$ and $D_\mu^0 D^+$ components, although we do not distinguish them here since we will use isospin-averaged masses. The value of the coupling constant $g_{T_{cc}DD^*}$ is chosen according to the analysis based on the compositeness condition performed in Ref. [23], in which for a size parameter α between 1.0 GeV and 2.0 GeV it is $g_{T_{cc}DD^*} = 6.17 - 6.40$ GeV.

The effective Lagrangians introduced above allow us to determine the amplitudes of the processes shown in Fig. 1. They are given by

$$\begin{aligned} \mathcal{M}_{T_{cc}\pi \rightarrow DD} &= \mathcal{M}_{T_{cc}^+}^{(a)} + \mathcal{M}_{T_{cc}^+}^{(b)}, \\ \mathcal{M}_{T_{cc}\pi \rightarrow D^* D^*} &= \mathcal{M}_{T_{cc}^+}^{(c)} + \mathcal{M}_{T_{cc}^+}^{(d)}, \\ \mathcal{M}_{T_{cc}\rho \rightarrow D^* D} &= \mathcal{M}_{T_{cc}^+}^{(e)} + \mathcal{M}_{T_{cc}^+}^{(f)}, \\ \mathcal{M}_{T_{cc}\pi \rightarrow DD^*} &= \mathcal{M}_{T_{cc}^+}^{(g)}, \\ \mathcal{M}_{T_{cc}\rho \rightarrow DD} &= \mathcal{M}_{T_{cc}^+}^{(h)} + \mathcal{M}_{T_{cc}^+}^{(i)}, \\ \mathcal{M}_{T_{cc}\rho \rightarrow D^* D^*} &= \mathcal{M}_{T_{cc}^+}^{(j)} + \mathcal{M}_{T_{cc}^+}^{(k)}, \end{aligned} \quad (4)$$

where the explicit expressions are

$$\begin{aligned} \mathcal{M}_{T_{cc}^+}^{(a)} &\equiv g_{T_{cc}DD^*} g_{\pi DD^*} \epsilon_1^\mu \frac{1}{t-m_D^{*2}} \\ &\quad \times \left(-g_{\mu\nu} + \frac{(p_1-p_3)_\mu (p_1-p_3)_\nu}{m_D^{*2}} \right) (p_2+p_4)^\nu, \\ \mathcal{M}_{T_{cc}^+}^{(b)} &\equiv -g_{T_{cc}DD^*} g_{\pi DD^*} \epsilon_1^\mu \frac{1}{u-m_D^{*2}} \\ &\quad \times \left(-g_{\mu\nu} + \frac{(p_1-p_4)_\mu (p_1-p_4)_\nu}{m_D^{*2}} \right) (p_2+p_3)^\nu, \\ \mathcal{M}_{T_{cc}^+}^{(c)} &\equiv -g_{T_{cc}DD^*} g_{\pi DD^*} \epsilon_1^\mu \epsilon_4^\nu \epsilon_{3\mu}^* \frac{1}{t-m_D^2} (2p_2-p_4)_\nu, \\ \mathcal{M}_{T_{cc}^+}^{(d)} &\equiv -g_{T_{cc}DD^*} g_{\pi DD^*} \epsilon_1^\mu \epsilon_3^\nu \epsilon_{4\mu}^* \frac{1}{u-m_D^2} (2p_2-p_3)_\nu, \\ \mathcal{M}_{T_{cc}^+}^{(e)} &\equiv -g_{T_{cc}DD^*} g_{\rho DD^*} \epsilon_1^\mu \epsilon_2^\nu \epsilon_{3\mu}^* \frac{1}{t-m_D^2} (2p_4-p_2)_\nu, \\ \mathcal{M}_{T_{cc}^+}^{(f)} &\equiv -g_{T_{cc}DD^*} g_{\rho D^* D^*} \epsilon_1^\mu \epsilon_2^\alpha \epsilon_3^\beta \frac{1}{u-m_{D^*}^2} \\ &\quad \times \left(-g_{\mu\nu} + \frac{(p_1-p_4)_\mu (p_1-p_4)_\nu}{m_{D^*}^2} \right) \\ &\quad \times ((2p_3-p_2)_\alpha g_{\beta\nu}^\nu - (p_3+p_2)^\nu g_{\alpha\beta} + (2p_2-p_3)_\beta g_\alpha^\nu), \\ \mathcal{M}_{T_{cc}^+}^{(g)} &\equiv g_{\pi D^* D^*} g_{T_{cc}DD^*} \epsilon_1^\mu \epsilon_4^\alpha \frac{1}{t-m_{D^*}^2} \epsilon_{\mu\nu\alpha\beta} p_2^\nu p_4^\beta, \\ \mathcal{M}_{T_{cc}^+}^{(h)} &\equiv g_{\rho DD^*} g_{T_{cc}DD^*} \epsilon_1^\mu \epsilon_2^\alpha \frac{1}{t-m_{D^*}^2} \\ &\quad \times \left(-g_{\mu\nu} + \frac{(p_1-p_3)_\mu (p_1-p_3)_\nu}{m_{D^*}^2} \right) \epsilon^{\nu\alpha\beta\gamma} p_{2\beta} p_{4\gamma}, \end{aligned} \quad (5)$$

and

$$\begin{aligned} \mathcal{M}_{T_{cc}^+}^{(i)} &\equiv -g_{\rho DD^*} g_{T_{cc}DD^*} \epsilon_1^\mu \epsilon_{2\alpha}^* \frac{1}{u-m_{D^*}^2} \\ &\quad \times \left(-g_{\mu\nu} + \frac{(p_1-p_4)_\mu (p_1-p_4)_\nu}{m_{D^*}^2} \right) \epsilon^{\nu\alpha\beta\gamma} p_{2\beta} p_{3\gamma}, \\ \mathcal{M}_{T_{cc}^+}^{(j)} &\equiv -g_{\rho DD^*} g_{T_{cc}DD^*} \epsilon_1^\mu \epsilon_{3\mu}^* \epsilon_2^\nu \epsilon_4^\alpha \frac{1}{t-m_D^2} \epsilon_{\nu\alpha\beta\gamma} p_2^\beta p_4^\gamma, \\ \mathcal{M}_{T_{cc}^+}^{(k)} &\equiv g_{\rho DD^*} g_{T_{cc}DD^*} \epsilon_1^\mu \epsilon_{4\mu}^* \epsilon_2^\nu \epsilon_3^\alpha \frac{1}{u-m_D^2} \epsilon_{\nu\alpha\beta\gamma} p_2^\beta p_3^\gamma. \end{aligned} \quad (6)$$

In the above equations, p_1 and p_2 are the momenta of initial state particles, while p_3 and p_4 are those of final state particles; $\epsilon_i^\mu \equiv \epsilon^\mu(p_i)$ is the polarization vector related to the respective vector particle i ; t and u are the Mandelstam variables, which together with the s -variable they are defined as: $s = (p_1+p_2)^2$, $t = (p_1-p_3)^2$, and $u = (p_1-p_4)^2$.

We define the total isospin-spin-averaged cross section in the center of mass (CM) frame for the processes in Eq. (4) as

$$\sigma_{ab \rightarrow cd} = \frac{1}{64\pi^2 s} \frac{|\vec{p}_{cd}|}{|\vec{p}_{ab}|} \int d\Omega \overline{\sum_{S,I}} |\mathcal{M}_{ab \rightarrow cd}|^2, \quad (7)$$

where $ab \rightarrow cd$ designates the reaction according to Eq. (4); \sqrt{s} denotes the CM energy; $|\vec{p}_{ab}|$ and $|\vec{p}_{cd}|$ are the three-momenta of initial and final particles in the CM frame, respectively; $d\Omega = d\phi d(\cos(\theta))$ is the solid angle measure; the symbol $\overline{\sum_{S,I}}$ stands for the sum over the spins and isospins of the particles, weighted by the isospin and spin degeneracy factors of the two particles forming the initial state, i.e. [30]

$$\overline{\sum_{S,I}} |\mathcal{M}_{ab \rightarrow cd}|^2 \rightarrow \frac{1}{g_a} \frac{1}{g_b} \sum_{S,I} |\mathcal{M}_{ab \rightarrow cd}|^2, \quad (8)$$

with $g_a = (2I_a+1)(2S_a+1)$ and $g_b = (2I_b+1)(2S_b+1)$ are the degeneracy factors of the particles in the initial state. In the present analysis we do not consider isospin violation.

The cross sections of the inverse processes, in which T_{cc}^+ is produced, can be calculated using the detailed balance relation, i.e.

$$g_a g_b |\vec{p}_{ab}|^2 \sigma_{ab \rightarrow cd}(s) = g_c g_d |\vec{p}_{cd}|^2 \sigma_{cd \rightarrow ab}(s). \quad (9)$$

Finally, in the implementation of the numerical calculations another ingredient should be brought into play. To avoid the artificial increase of the amplitudes with the CM energy, we include a Gaussian form factor for each vertex present in a given diagram, namely [35]:

$$F = \exp\left(-\frac{(q^2 - m_{ex}^2)^2}{\Lambda^4}\right), \quad (10)$$

where q is the four-momentum of the exchanged particle of mass m_{ex} for a vertex involving a t - or u -channel meson exchange. We note that the choice of the form factor and of an appropriate cutoff value is arbitrary (we refer

the reader to Ref. [35] for a detailed discussion). The usual procedure is to take some experimental data as input to fix them. In this sense, it can be noticed that in most of the cases the chosen form factors are monopole, dipole or exponential-like, and the used cutoff values are of the order of $m_{min} < \Lambda < m_{max}$, where m_{min} (m_{max}) is the mass of the lightest (heaviest) particle entering or exiting the vertex. Furthermore, it is worth mentioning that in Ref. [23] a nonlocal vertex involving the T_{cc}^+ state is described in terms of the Weinberg compositeness condition; a function F with an exponential form appears as an effective correlation function to reflect the distribution of two constituents of a bound state system, as well as to make the amplitudes ultraviolet finite. Thus, we believe that the choice in Eq. (10) sounds reasonable.

III. RESULTS AND DISCUSSION

In this Section we will evaluate and discuss the doubly-charmed state absorption and production cross sections calculated previously. The computations of the present work are done with the isospin-averaged masses for the light and heavy mesons reported in Ref. [38]: $m_\pi = 137.28$ MeV, $m_\rho = 775.38$ MeV, $m_{\bar{D}} = 1867.24$ MeV and $m_{\bar{D}^*} = 2008.56$ MeV; for the T_{cc}^+ we use $m_{T_{cc}^+} = 3874.75$ MeV [1, 2]. The cutoff Λ is chosen to be in the range 2500 – 3700 MeV. In this kind of calculation the cutoff is the most important source of uncertainty. Because we use a range of values (instead of a single number) for the cutoff, our results will be given with uncertainty bands. We note that the uncertainty associated with the cutoff is much larger than the one related to the coupling constant, which is not shown in the plots. This is a conservative procedure which tends to overestimate the theoretical error. In spite of these uncertainties we can still draw conclusions from our calculations.

Plots of the cross sections as functions of the CM energy \sqrt{s} for the T_{cc}^+ -absorption by pion or ρ mesons are shown in Fig. 2. Upper and lower limits of the bands are obtained taking the upper (3.7 GeV) and lower (2.5 GeV) limits of the cutoff.

Since all these absorption cross sections are exothermic (except the one for $T_{cc}^+ \pi \rightarrow D^*D^*$), they become very large at the threshold. In the case of $\sigma_{T_{cc}^+ \pi \rightarrow D^*D^*}$, the behavior is not totally shown in the plot. The initial and final states have a small difference, and suffer a fast increase very close to the D^*D^* mass and a decrease after that. We note that in the region close to the threshold the corresponding curves obtained with and without form factors are indistinguishable (we do not display another Figure proving this for the sake of conciseness).

The results suggest that within the range $4.05 \leq \sqrt{s} \leq 4.5$ GeV, $\sigma_{T_{cc}^+ \pi \rightarrow X}$ ($X = DD, DD^*, D^*D^*$) have distinct magnitudes, being of order of $\sim 10^{-1} - 10$ mb. It can be noticed that $\sigma_{T_{cc}^+ \pi \rightarrow DD}$ is suppressed with respect to the other processes, at least by one order of magnitude. However, at higher CM energies ($5 \leq \sqrt{s} \leq 5.5$ GeV), all

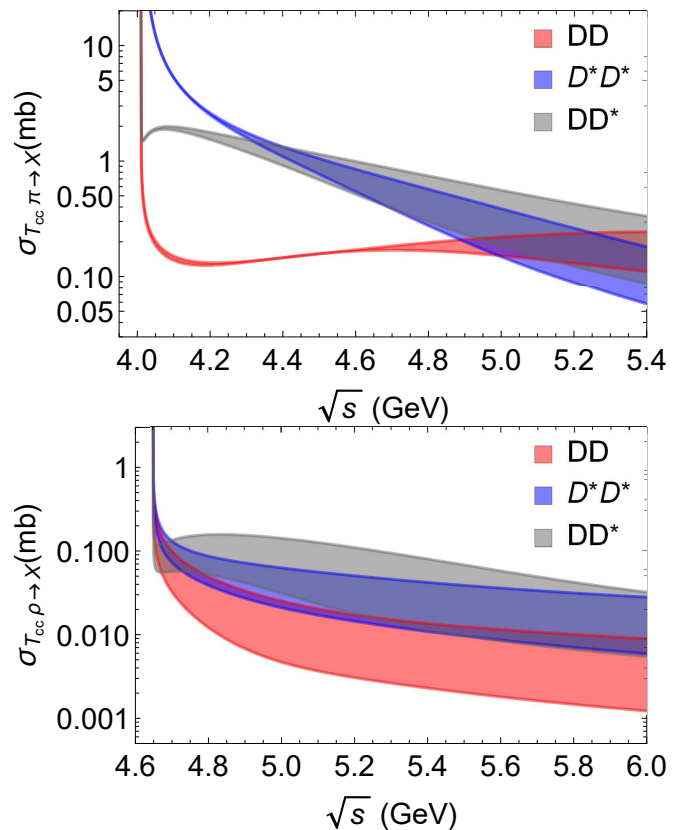


FIG. 2. Cross sections for the absorption processes $T_{cc}^+ \pi \rightarrow D^{(*)}D^{(*)}$ (top panel) and $T_{cc}^+ \rho \rightarrow D^{(*)}D^{(*)}$ (bottom panel), as functions of the CM energy \sqrt{s} . Upper and lower limits of the band are obtained taking the upper (3.7 GeV) and lower (2.5 GeV) limits of the cutoff.

the processes have similar magnitudes.

Looking now at the absorption processes by a ρ meson, which occur at higher thresholds, the $\sigma_{T_{cc}^+ \rho \rightarrow D^*D}$ is the biggest at moderate energies, while the cross section for DD final states is the smallest. When we compare the different dissociation processes at a given CM energy, for instance $\sqrt{s} = 5$ GeV, we observe that $\sigma_{T_{cc}^+ \pi \rightarrow X}$ are greater than the respective $\sigma_{T_{cc}^+ \rho \rightarrow X}$ by about one order of magnitude. These findings allow to quantitatively estimate how big is the contribution coming from the doubly-charmed state absorption by a pion with respect to the other reactions.

Now let us move on the T_{cc}^+ -production cross sections, which are shown in Fig. 3 as functions of the CM energy. Except for $\sigma_{D^*D^* \rightarrow T_{cc}^+ \pi}$, they are endothermic, with magnitudes of the order $\sim 10^{-3} - 10^{-1}$ mb, within the range of CM energies considered. In general, the comparison with the outputs reported in Fig. 2 reveals that both $T_{cc}^+ \pi$ and $T_{cc}^+ \rho$ absorption cross sections are greater than the respective production ones. We mention that this fact is engendered by the kinematic effects encoded in the detailed balance relations.

Finally, in Fig. 4 we compare our results with those obtained in Ref. [11]. As it can be seen from the figure, our

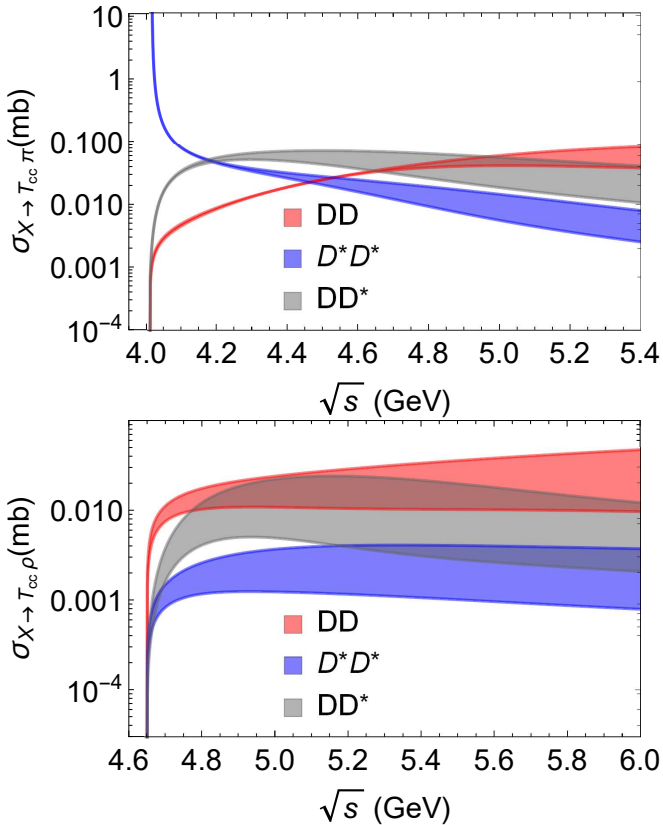


FIG. 3. Cross sections as functions of the CM energy \sqrt{s} for the respective inverse (production) processes displayed in Fig. 2, i.e. $D^{(*)}D^{(*)} \rightarrow T_{cc}^+\pi$ (top panel) and $D^{(*)}D^{(*)} \rightarrow T_{cc}^+\rho$ (bottom panel), obtained via the detailed balance relation. Upper and lower limits of the bands are obtained taking the upper (3.7 GeV) and lower (2.5 GeV) limits of the cutoff.

cross sections are significantly smaller than those found in [11]. In comparison to the effective Lagrangian adopted here, in the quasi-free approximation the T_{cc}^+ is “too easy to destroy”. Part of this difference can be attributed to the form factors used in each work. We have employed an exponential form factor, whereas in [11] the authors use a monopole form factor. The former suppresses more strongly the cross section than the latter.

The results reported above show that the T_{cc}^+ absorption in a hadron gas is more pronounced than its production. This result is not surprising and a similar dominance of absorption over production was found in the case of J/ψ , Υ , and other multiquark states such as the $X(3872)$ and Z_b .

Once the vacuum cross sections are known, the next step is to compute the thermal cross sections, which are convolutions of the vacuum cross sections with thermal momentum distributions of the colliding particles. In this approach, the temperature of the hadron gas (which is in the range 100 - 200 MeV) determines the collision energy. When we perform this thermal average, the kinematical configurations close to the thresholds are highly

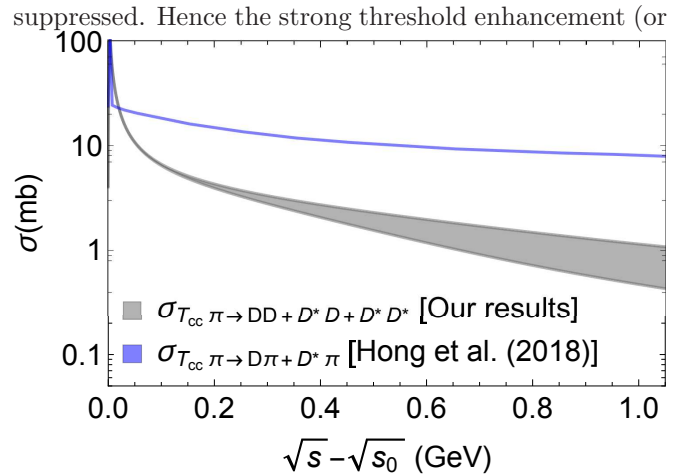


FIG. 4. Cross sections $T_{cc}^+\pi$ obtained in this work and in Ref. [11].

suppression) observed in all the figures above have little significance for applications to heavy ion collisions.

IV. CONCLUDING REMARKS

The purpose of this work was to study the absorption and production processes involving the recently observed doubly charmed tetraquark state T_{cc}^+ in a hadronic medium. We considered the reactions $T_{cc}^+\pi, T_{cc}^+\rho \rightarrow D^{(*)}D^{(*)}$ and the corresponding inverse ones. We have used effective Lagrangians to account for the dynamics of the hadrons involved and we have computed the relevant cross sections. This is the first calculation of this kind for the T_{cc}^+ . So far the only existing estimate of the T_{cc}^+ absorption cross section, published in Ref. [11], was based on the quasi-free approximation. In our approach we obtain much smaller absorption cross sections.

The total cross sections for the dissociation reactions have been estimated, as well as their inverse processes using the detailed balance principle. The results suggest sizeable cross sections for the considered processes. Moreover, the T_{cc}^+ absorption in a hadron gas appears to be more important than its production.

The obtained T_{cc}^+ production and absorption cross sections will be crucial for a comprehensive analysis of the evolution of the T_{cc}^+ abundance in heavy ion collisions. This is another observable useful to shed light on the T_{cc}^+ internal structure. This study is in progress and we expect to publish it soon.

ACKNOWLEDGMENTS

The authors would like to thank the Brazilian funding agencies for their financial support: CNPq (LMA: contracts 309950/2020-1 and 400546/2016-7) and FAPESB (LMA: contract INT0007/2016).

-
- [1] R. Aaij *et al.* [LHCb], [arXiv:2109.01038 [hep-ex]].
- [2] R. Aaij *et al.* [LHCb], [arXiv:2109.01056 [hep-ex]].
- [3] B. A. Gelman and S. Nussinov, *Phys. Lett. B* **551**, 296 (2003).
- [4] D. Janc and M. Rosina, *Few Body Syst.* **35**, 175 (2004).
- [5] J. Vijande, F. Fernandez, A. Valcarce and B. Silvestre-Brac, *Eur. Phys. J. A* **19**, 383 (2004).
- [6] F. S. Navarra, M. Nielsen and S. H. Lee, *Phys. Lett. B* **649**, 166 (2007).
- [7] J. Vijande, E. Weissman, A. Valcarce and N. Barnea, *Phys. Rev. D* **76**, 094027 (2007).
- [8] D. Ebert, R. N. Faustov, V. O. Galkin and W. Lucha, *Phys. Rev. D* **76**, 114015 (2007).
- [9] S. H. Lee and S. Yasui, *Eur. Phys. J. C* **64**, 283 (2009).
- [10] Y. Yang, C. Deng, J. Ping and T. Goldman, *Phys. Rev. D* **80**, 114023 (2009).
- [11] J. Hong, S. Cho, T. Song and S. H. Lee, *Phys. Rev. C* **98**, 014913 (2018).
- [12] R. J. Hudspith, B. Colquhoun, A. Francis, R. Lewis and K. Maltman, *Phys. Rev. D* **102**, 114506 (2020).
- [13] J. B. Cheng, S. Y. Li, Y. R. Liu, Z. G. Si and T. Yao, *Chin. Phys. C* **45**, 043102 (2021).
- [14] Q. Qin, Y. F. Shen and F. S. Yu, *Chin. Phys. C* **45**, 103106 (2021).
- [15] S. S. Agaev, K. Azizi and H. Sundu, [arXiv:2108.00188 [hep-ph]].
- [16] X. K. Dong, F. K. Guo and B. S. Zou, [arXiv:2108.02673 [hep-ph]].
- [17] Y. Huang, H. Q. Zhu, L. S. Geng and R. Wang, [arXiv:2108.13028 [hep-ph]].
- [18] N. Li, Z. F. Sun, X. Liu and S. L. Zhu, *Chin. Phys. Lett.* **38**, 092001 (2021).
- [19] H. Ren, F. Wu and R. Zhu, [arXiv:2109.02531 [hep-ph]].
- [20] Q. Xin and Z. G. Wang, [arXiv:2108.12597 [hep-ph]].
- [21] G. Yang, J. Ping and J. Segovia, [arXiv:2109.04311 [hep-ph]].
- [22] L. Meng, G. J. Wang, B. Wang and S. L. Zhu, *Phys. Rev. D* **104**, 051502 (2021).
- [23] X. Z. Ling, M. Z. Liu, L. S. Geng, E. Wang and J. J. Xie, [arXiv:2108.00947 [hep-ph]].
- [24] S. Fleming, R. Hodges and T. Mehen, [arXiv:2109.02188 [hep-ph]].
- [25] Y. Jin, S. Y. Li, Y. R. Liu, Q. Qin, Z. G. Si and F. S. Yu, [arXiv:2109.05678 [hep-ph]].
- [26] K. Azizi and U. Özdem, [arXiv:2109.02390 [hep-ph]].
- [27] Y. Hu, J. Liao, E. Wang, Q. Wang, H. Xing and H. Zhang, [arXiv:2109.07733 [hep-ph]].
- [28] L. W. Chen, C. M. Ko, W. Liu and M. Nielsen, *Phys. Rev. C* **76**, 014906 (2007); F. S. Navarra, M. Nielsen, M. E. Bracco, M. Chiapparini and C. L. Schat, *Phys. Lett. B* **489**, 319 (2000); F. S. Navarra, M. Nielsen and M. E. Bracco, *Phys. Rev. D* **65**, 037502 (2002).
- [29] S. Cho and S. H. Lee, *Phys. Rev. C* **88**, 054901 (2013); M. E. Bracco, M. Chiapparini, F. S. Navarra and M. Nielsen, *Phys. Lett. B* **659**, 559 (2008).
- [30] A. Martínez Torres, K. P. Khemchandani, F. S. Navarra, M. Nielsen and L. M. Abreu, *Phys. Rev. D* **90**, 114023 (2014); A. Martínez Torres, K. P. Khemchandani, F. S. Navarra, M. Nielsen and L. M. Abreu, *Acta Phys. Pol. B Proc. Supp.* **8**, 247 (2015).
- [31] L. M. Abreu, K. P. Khemchandani, A. Martínez Torres, F. S. Navarra and M. Nielsen, *Phys. Lett. B* **761**, 303 (2016).
- [32] L. M. Abreu, K. P. Khemchandani, A. Martínez Torres, F. S. Navarra, M. Nielsen and A. L. Vasconcellos, *Phys. Rev. D* **95**, 096002 (2017).
- [33] A. Martínez Torres, K. P. Khemchandani, L. M. Abreu, F. S. Navarra and M. Nielsen, *Phys. Rev. D* **97**, 056001 (2018).
- [34] L. M. Abreu, K. P. Khemchandani, A. Martínez Torres, F. S. Navarra and M. Nielsen, *Phys. Rev. C* **97**, 044902 (2018).
- [35] L. M. Abreu, F. S. Navarra and M. Nielsen, *Phys. Rev. C* **101**, 014906 (2020).
- [36] C. Le Roux, F. S. Navarra and L. M. Abreu, *Phys. Lett. B* **817**, 136284 (2021).
- [37] S. G. Matinyan and B. Müller, *Phys. Rev. C* **58**, 2994 (1998); Y. Oh, T. Song and S. H. Lee, *Phys. Rev. C* **63**, 034901 (2001); F. Carvalho, F. O. Duraes, F. S. Navarra and M. Nielsen, *Phys. Rev. C* **72**, 024902 (2005); B. Osorio Rodrigues, M. E. Bracco, M. Nielsen and F. S. Navarra, *Nucl. Phys. A* **852**, 127 (2011).
- [38] P. A. Zyla *et al.* [Particle Data Group], *PTEP* **2020**, 083C01 (2020).
- [39] S. Baines, N. E. Mavromatos, V. A. Mitsou, J. L. Pinfold and A. Santra, *Eur. Phys. J. C* **78**, 966 (2018); [erratum: *Eur. Phys. J. C* **79**, 166 (2019)].